Heterogeneous Catalytic Oxidation

DOI: 10.1002/anie.200603144

Supported Pt–Co Catalysts for Selective CO Oxidation in a Hydrogen-Rich Stream**

Eun-Yong Ko, Eun Duck Park, Hyun Chul Lee,* Doohwan Lee, and Soonho Kim*

The polymer electrolyte membrane fuel cell (PEMFC) has come to be regarded as one of the most promising candidates for utilizing hydrogen to produce heat and electricity, especially for electric vehicles or residential co-generation systems.[1] Pt and Pt-based alloys, which are generally used as the anode of PEMFCs, are known to be easily poisoned by even small amounts of CO in the hydrogen-rich stream that can be produced from various hydrocarbons by the reforming and water gas shift (WGS) reactions.[2] Due to the limited catalytic activities of the current WGS catalysts for complete CO conversion, which is thermodynamically favored at low temperatures, approximately 0.5–1 vol% of unconverted CO remains in the effluent, and this should be removed to a trace level of below 10 ppm before reaching the PEMFC. Among the methods proposed to remove this residual CO, preferential CO oxidation (PROX) has been accepted as one of the most promising.[2] Three main reactions take place in this system. The reaction that competes most effectively with CO oxidation [Eq. (1)] is H_2 oxidation [Eq. (2)] because of the H_2-rich conditions in the gas stream in practical fuel cell applications. In addition, CO can consume additional H_2 by undergoing hydrogenation [Eq. (3)], a process also known as methanation, which should be avoided unless the CO concentration in the reactant stream is quite low, because it consumes relatively large amounts of hydrogen (3 mol per mol CO).

$$CO + 1/2\,O_2 \rightarrow CO_2 \quad (1)$$

$$H_2 + 1/2\,O_2 \rightarrow H_2O \quad (2)$$

$$CO + 3\,H_2 \rightarrow CH_4 + H_2O \quad (3)$$

Thus, a highly active and selective catalyst is required to remove CO from the H_2-rich stream before it reaches the PEMFC. Among a number of catalysts reported to be active for PROX,[3] supported platinum catalysts have been considered to be promising in view of their high catalytic performance. However, they usually only show noticeable activities under practical conditions above 423 K,[3a] where the reverse WGS reaction could occur, thereby hindering complete CO removal. Many researchers have therefore made efforts to enhance the PROX activity of supported platinum catalysts at low temperatures, for example by water vapor pre-treatment of the Pt catalyst,[3b] the addition of alkali metals,[3c] and the addition of other metals.[3d–n] In a previous study, we found that Pt–Co/γ-Al_2O_3 is one of the most active catalysts among the supported Pt catalysts tested under the same reaction conditions.[3k,l] Until now, most work has been conducted on Pt-based catalysts supported on γ-Al_2O_3, and the effect of supports on Pt-based catalysts has been limited to TiO_2[3m] and CeO_2.[3n] Furthermore, the Pt loading in some active Pt-based catalysts is relatively high, which can hinder their practical applications.[3b,e–g]

Herein, we report that a Pt–Co bimetallic catalyst supported on yttria-stabilized zirconia (YSZ) is highly efficient for PROX in a H_2-rich gas stream even with a small amount of Pt (0.5 wt%) at temperatures below 423 K. By optimizing the calcination and reduction pre-treatment conditions for Pt–Co/YSZ, the CO concentration can be decreased below 10 ppm in the temperature range 380–423 K. Furthermore, an isolated Pt–Co bimetallic phase can be observed on this catalyst.

Figure 1 shows the catalytic performance of Pt–Co/YSZ for PROX with increasing reaction temperatures. An extremely high H_2 concentration (80 vol%) in the reactant stream was adopted. The BET surface area of the YSZ employed, as determined by N_2 adsorption isotherms, was $9\ m^2\,g^{-1}$. As shown in Figure 1, Pt–Co/YSZ catalysts reveal much higher activity and selectivity for PROX compared with those of the unpromoted Pt/YSZ catalyst at all reaction temperatures. For the Pt/YSZ catalyst, the CO conversion and CO_2 selectivity at temperatures above 423 K were about 40% and 20%, respectively. The addition of Co to Pt/YSZ resulted in a large enhancement in catalytic performance for PROX, especially in the temperature region below 423 K. However, the extent of the increase of CO and O_2 conversion depends on the preparation conditions. Thus, as the amount of Pt decreases from 1.0 to 0.5 wt% in Pt–Co/YSZ, the reaction temperature showing the maximum PROX activity is shifted to higher temperature by approximately 60 K.

[*] E.-Y. Ko, Prof. Dr. E. D. Park
Division of Energy Systems Research and
Division of Chemical Engineering and Materials Engineering
Ajou University
Wonchun-Dong, Yeongtong-Gu
Suwon, 443-749 (Republic of Korea)
Fax: (+82) 31-219-1612
E-mail: edpark@ajou.ac.kr
Homepage: http://home.ajou.ac.kr/homesite/green/
Dr. H. C. Lee, Dr. D. Lee, Dr. S. Kim
Energy & Materials Research Laboratory
Samsung Advanced Institute of Technology (SAIT)
P.O. Box 111, Suwon, 440-600 (Republic of Korea)
Fax: (+82) 31-280-9359
E-mail: hc001.lee@samsung.com

[**] This work was supported by the Samsung Advanced Institute of Technology (SAIT).

Supporting Information for this article is available on the WWW under http://www.angewandte.org or from the author.

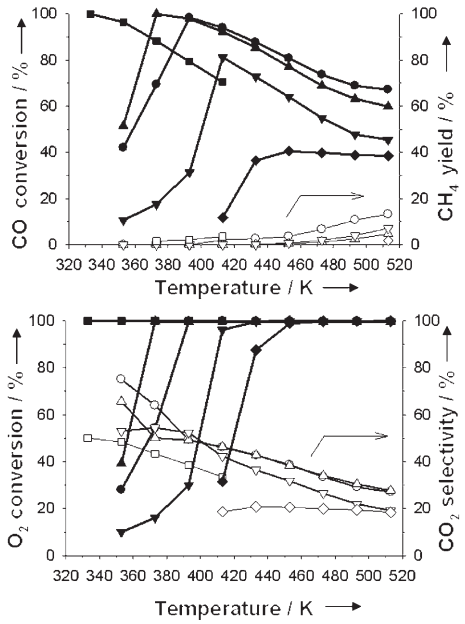

Figure 1. PROX over Pt/YSZ and Pt–Co/YSZ catalysts with increasing reaction temperature at a ramping rate of 1 K min^{-1}. Catalyst preparation: 0.5 wt% Pt–Co/YSZ (Co/Pt = 5) calcined and reduced at 573 K (●, ○) or 773 K (▲, △); 0.5 wt% Pt–Co/YSZ (Co/Pt = 5) calcined at 973 K and reduced at 773 K (▼, ▽); 1 wt% Pt–Co/YSZ (Co/Pt = 10) calcined and reduced at 573 K (■, □); and 1 wt% Pt/YSZ calcined and reduced at 573 K (◆, ◇). Reaction conditions: 1 vol% CO, 1 vol% O_2, 80 vol% H_2, and 2 vol% H_2O in He. F/W = 1000 mL min^{-1} (g cat)$^{-1}$. F/W: ratio of the total gaseous reactant flow rate to the catalyst weight.

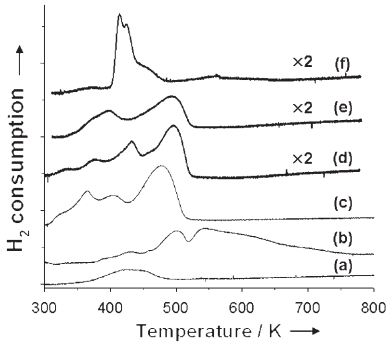

Figure 2. TPR curves of Co-promoted Pt/YSZ catalysts: a) 1 wt% Pt/YSZ, b) 3 wt% Co/YSZ, or c) 1 wt% Pt–Co/YSZ (Co/Pt = 10) calcined at 573 K; 0.5 wt% Pt–Co/YSZ (Co/Pt = 5) catalysts calcined at d) 573 K, e) 773 K, or f) 973 K. For clarity, the curves are shifted vertically.

The influence of the pre-treatment conditions for Pt–Co/YSZ containing 0.5 wt% Pt on the catalytic activity for PROX is also revealed by Figure 1. With an increase of the calcination and reduction temperature from 573 to 773 K, the maximum CO conversion is obtained at slightly lower temperature; CH_4 formation decreases at all reaction temperatures. A calcination temperature higher than 773 K results in a rapid decrease in both CO conversion and CO_2 selectivity. Thus, the most active Pt–Co/YSZ catalyst for PROX was found to be that calcined and reduced at 773 K, where the amount of Pt can be reduced to 0.5 wt% whilst maintaining high catalytic performance. Furthermore, the Co/Pt molar ratio can be adjusted from 5 to 20 to be effective for PROX and the Pt–Co/YSZ catalyst shows higher catalytic activity at temperatures below 423 K than other Pt–Co catalysts supported on γ-Al_2O_3, SiO_2, or TiO_2 under the same reaction conditions.[4]

Temperature-programmed reduction (TPR) was conducted to try to determine the interactions between Pt and Co, as well as those between Pt, Co oxides (CoOx), and YSZ (Figure 2). YSZ is well known to be a reducible support with surface oxygen vacancies.[5] For CO oxidation, it has been proposed that the lattice oxygen and interfacial metal–support interaction play a crucial role in promoting CO oxidation when metal species are supported on an oxygen-ion-conducting support.[5,6] As shown in Figure 2a, the sample with 1 wt% Pt/YSZ leads to one broad reduction peak at around 440 K, which could be related to the reduction of platinum oxide into Pt metal. The 3 wt% Co/YSZ sample (Figure 2b) exhibits two adjacent reduction peaks for Co oxides with maxima at 500 and 540 K. This reduction occurs until the temperature reaches 760 K, thus indicating that different metal–support interactions exist between Co oxides and YSZ. The 1 wt% Pt–Co/YSZ sample (Co/Pt = 10, in which the amount of Co is 3 wt%; Figure 2c) shows three adjacent reduction peaks with maxima at 365, 400, and 475 K. These reduction temperatures are much lower than those of the 1 wt% Pt/YSZ and 3 wt% Co/YSZ samples. The lowest temperature peak could be due to the reduction of newly created bimetallic Pt–Co oxides and the others to the reduction of cobalt oxides to metallic Co.

A similar TPR pattern was observed for the 0.5 wt% Pt–Co/YSZ sample calcined at 573 K, with a 30-K shift of the peaks to higher temperatures and with a continuous reduction signal up to 773 K (Figure 2d). For the most active catalyst (sample calcined at 773 K; Figure 2e), the reduction peak at 430 K in Figure 2d has disappeared, thus indicating that the Co oxide is uniformly formed at a higher calcination temperature, as shown in the TEM images in Figures 3c,d. However, for the catalyst calcined at 973 K, disappearance of the bimetallic Pt–Co reduction peak at low temperatures and overlap of the reduction peaks from Co oxides occurs, as shown in Figure 2f. The low catalytic activity of this catalyst (Figure 1) appears to be related to the disappearance of the Pt–Co bimetallic peak.

To observe the nanosized bimetallic Pt–Co phase, TEM images were obtained for the 0.5 wt% Pt–Co/YSZ (Co/Pt = 5) catalysts calcined and reduced at different temperatures (Figure 3). Interestingly, the Pt–Co/YSZ catalyst calcined and reduced at 773 K, which is the most active catalyst for PROX, shows a distinct distribution of isolated Pt–Co bimetallic nanoparticles with an average size of (2.9 ± 0.5) nm along with isolated Co particles, as shown in Figures 3c,d. The Pt–Co/YSZ catalyst calcined and reduced at 573 K shows bimetallic Pt–Co nanoparticles embedded in Co oxides along with isolated Pt–Co bimetallic particles, whereas core–shell-structured Pt–Co and Co particles were found for the catalyst calcined at 973 K and reduced at 773 K. In light of these results, the presence of bimetallic Pt–Co nanoparticles

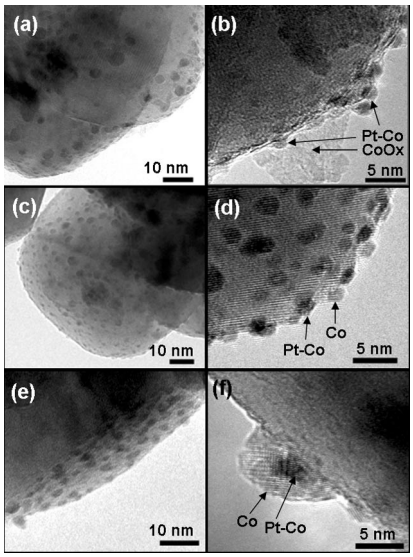

Figure 3. Bright-field TEM images of the 0.5 wt% Pt–Co/YSZ catalyst (Co/Pt = 5) calcined in air and reduced in H_2 at different temperatures: a,b) calcined and reduced at 573 K; c,d) calcined and reduced at 773 K; e,f) calcined at 973 K and reduced at 773 K.

in contact with a reducible support having surface oxygen vacancies could be the reason for the high PROX activity of the Pt–Co/YSZ catalyst. The presence of a bimetallic Pt–Co phase such as Pt_3Co or PtCo has also been reported in other catalyst systems.[7] In the case of the Pt–Co/YSZ catalysts, we also found by energy-dispersive X-ray (EDX) analysis of different regions that the ratio of Co to Pt is below one for the sample calcined and reduced at 573 K and below 1.5 for the sample calcined and reduced at 773 K, both of which are active catalysts containing Pt–Co bimetallic nanoparticles that interact with the YSZ support. However, for the sample calcined at 973 K, we found that Co nanoparticles cover most of the surface of the support and the Co/Pt ratio in the core–shell structure exceeds six, which results in low PROX activity.[4] Therefore, it is reasonable to conclude that the formation of isolated bimetallic Pt–Co nanoparticles is responsible for the high PROX activity.

An investigation of these catalysts for PROX under practical conditions (an excess H_2 gas stream containing CO_2 and a large amount of H_2O) was carried out to confirm the high catalytic performance of the selected compound, that is, that calcined and reduced at 773 K. As shown in Figure 4, the Pt–Co/YSZ catalyst is highly effective for PROX as it reduces the CO concentration to below 10 ppm in the temperature range 380–423 K without any significant change in the H_2 and CO_2 concentrations.

In summary, the YSZ-supported Pt–Co catalyst reported here is highly active for PROX in a H_2-rich gas stream at temperatures below 423 K even with a small amount of Pt (0.5 wt%). Careful adjustment of the pre-treatment calcination and reduction conditions provides a Pt–Co/YSZ catalyst that can reduce the CO concentration to below 10 ppm in the temperature range 380–423 K. The presence of isolated bimetallic Pt–Co nanoparticles interacting with the support seems to give rise to this high catalytic activity.

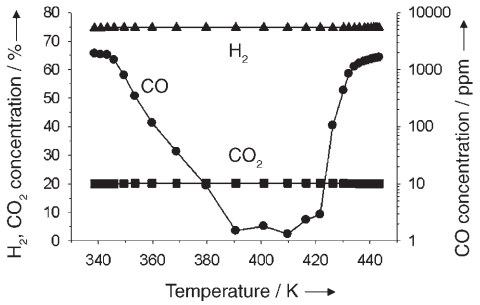

Figure 4. The steady-state H_2, CO_2, and CO concentrations based on the dry gas at different reaction temperatures over the 0.5 wt% Pt–Co/YSZ (Co/Pt = 10) catalyst calcined and reduced at 773 K. Reaction conditions: 0.9 vol% CO, 0.9 vol% O_2, 17.4 vol% CO_2, 64.6 vol% H_2, and 13 vol% H_2O in N_2. F/W = 278 mL min^{-1} (g cat)$^{-1}$.

Experimental Section

All the catalysts were prepared by a single-step, co-impregnation method from an aqueous solution of $[Pt(NH_3)_4](NO_3)_2$ and $Co(NO_3)_2$ over YSZ (TZ-8YS, Tosoh), followed by drying at 373 K for 12 h. The loading of Pt was varied from 0.2 to 1.0 wt% and the Co/Pt molar ratio was varied from 0 to 50. Calcination and reduction were carried out in air and a H_2 stream, respectively, at various temperatures. Temperature programmed reduction (TPR) was conducted with a 0.2-g sample in a 10 vol% H_2/Ar stream from 300 to 800 K at a heating rate of 10 K min^{-1}. The TCD signals were recorded after calcining the samples at different temperatures for 1 h. The bright-field TEM image was recorded with a Technai G^2 TEM (FEI) operating at 200 kV. Catalytic activity tests for PROX were carried out in a small, fixed-bed reactor with catalysts that had been retained between 45 and 80 mesh sieves. A standard gas containing 1.0 vol% CO, 1.0 vol% O_2, 2.0 vol% H_2O, and 80 vol% H_2 balanced with helium was used to compare the catalytic performance of the various catalysts. Subsequently, realistic gas flow conditions of 0.9 vol% CO, 0.9 vol% O_2, 17.4 vol% CO_2, 64.6 vol% H_2, and 13 vol% H_2O balanced with N_2 were adopted to confirm the catalytic performance for the most active catalyst. The reactant gas flow was fed into the reactor at atmospheric pressure. The conversion of CO and O_2 and the yield of CH_4 were determined by GC analysis (HP5890A, 5-Å molecular sieve column) of the effluent stream of the reactor. The detection limit of CO was 10 ppm. The effluent gas composition was also determined with an online gas analyzer (NGA2000, MLT4, Rosemount Analyzer System from Emerson Process Management; CO at ppm level, CO_2, H_2, and CH_4 at percent level). The conversion of CO and O_2 was calculated from the ratio of the amount consumed to the initial amount of each gas. The CH_4 yield was determined from the ratio of the amount of CH_4 produced to the initial CO amount. Finally, the CO_2 selectivity for PROX was defined as the ratio of the amount of O_2 consumed by CO oxidation to the total amount of O_2 consumed, as described elsewhere.[3k]

Received: August 3, 2006
Revised: October 23, 2006
Published online: December 8, 2006

Keywords: bimetallic catalysts · carbon monoxide · heterogeneous catalysis · oxidation · platinum

[1] C. Song, *Catal. Today* **2002**, *77*, 17.
[2] L. Shore, R. J. Farrauto in *Handbook of Fuel Cells: Fundamentals, Technology and Applications*, *Vol. 3*, *Part 2* (Eds.: W. Vielstich, A. Lamm, H. A. Gasteiger), Wiley, Chichester, **2003**, pp. 211–218.

[3] a) S. H. Oh, R. M. Sinkevitch, *J. Catal.* **1993**, *142*, 254; b) I. H. Son, M. Shamsuzzoha, A. M. Lane, *J. Catal.* **2002**, *210*, 460; c) Y. Minemura, S. Ito, T. Miyao, S. Naito, K. Tomishige, K. Kunimori, *Chem. Commun.* **2005**, 1429; d) O. Korotkikh, R. Farrauto, *Catal. Today* **2000**, *62*, 249; e) X. Liu, O. Korotkikh, R. Farrauto, *Appl. Catal. A* **2002**, *226*, 293; f) M. Watanabe, H. Uchida, K. Ohkubo, H. Igarashi, *Appl. Catal. B* **2003**, *46*, 595; g) A. Sirijaruphan, J. G. Goodwin, Jr., R. W. Rice, *J. Catal.* **2004**, *224*, 304; h) I. H. Son, A. M. Lane, *Catal. Lett.* **2001**, *76*, 151; i) D. J. Suh, C. Kwak, J.-H. Kim, S. M. Kwon, T.-J. Park, *J. Power Sources* **2005**, *142*, 70; j) E.-Y. Ko, E. D. Park, K. W. Seo, H. C. Lee, D. Lee, S. Kim, *Catal. Lett.* **2006**, *110*, 275; k) E.-Y. Ko, E. D. Park, K. W. Seo, H. C. Lee, D. Lee, S. Kim, *Korean J. Chem. Eng.* **2006**, *23*, 182; l) E.-Y. Ko, E. D. Park, K. W. Seo, H. C. Lee, D. Lee, S. Kim, *J. Nanosci. Nanotechnol.* **2006**, *6*, 3567; m) W. S. Epling, P. K. Cheekatamarla, A. M. Lane, *Chem. Eng. J.* **2003**, *93*, 61; n) O. Pozdnyakova, D. Teschner, A. Wootsch, J. Kröhnert, B. Steinhauer, H. Sauer, L. Toth, F. C. Jentoft, A. Knop-Gericke, Z. Paál, R. Schlögl, *J. Catal.* **2006**, *237*, 1.

[4] Detailed experimental results are available as Supporting Information.

[5] W.-P. Dow, T.-J. Huang, *J. Catal.* **1996**, *160*, 171.

[6] A. Katsaounis, Z. Nikopoulou, X. E. Verykios, C. G. Vayenas, *J. Catal.* **2004**, *226*, 197.

[7] a) S. Zyade, F. Garin, G. Maire, *Nouv. J. Chim.* **1987**, *11*, 429; b) Z. Zsoldos, T. Hoffer, L. Guczi, *J. Phys. Chem.* **1991**, *95*, 798.

